AD-A092 448 AIR FORCE GEOPHYSICS LAB HANSCOM AFB MA F/G 7/4
STRUCTURE AND COMPOSITION MEASUREMENTS IN EQUATORIAL IONOSPHERI--ETC(U)
JUL 80 R NARCISI, E TRZCINSKI, G FEDERICO
UNCLASSIFIED AFGL-TR-80-0222 NL

END
DATE FILMED
1-81
DTIC

LEVEL II

12

AFGL-TR-80-0222
ENVIRONMENTAL RESEARCH PAPERS, NO. 711

Structure and Composition Measurements in Equatorial Ionospheric Bubbles

R. NARCISI
E. TRZCINSKI
G. FEDERICO
L. WLODYKA
P. BENCH

9 July 1980

AERONOMY DIVISION PROJECT 2310
AIR FORCE GEOPHYSICS LABORATORY
HANSCOM AFB, MASSACHUSETTS 01731

AIR FORCE SYSTEMS COMMAND, USAF

This report has been reviewed by the ESD Information Office (OI) and is releasable to the National Technical Information Service (NTIS).

This technical report has been reviewed and
is approved for publication.

FOR THE COMMANDER

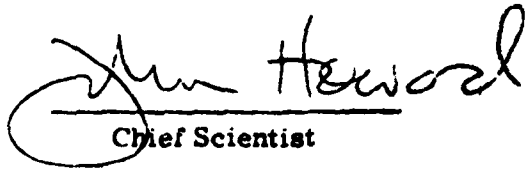

Chief Scientist

Qualified requestors may obtain additional copies from the Defense Technical Information Center. All others should apply to the National Technical Information Service.

(9) Final rept.,

Unclassified

SECURITY CLASSIFICATION OF THIS PAGE (When Data Entered)

REPORT DOCUMENTATION PAGE	READ INSTRUCTIONS BEFORE COMPLETING FORM
1. REPORT NUMBER: AFGL-TR-80-0222	2. GOVT ACCESSION NO.: AD-A092 448
3. RECIPIENT'S CATALOG NUMBER	
4. TITLE (and Subtitle): STRUCTURE AND COMPOSITION MEASUREMENTS IN EQUATORIAL IONOSPHERIC BUBBLES	5. TYPE OF REPORT & PERIOD COVERED: Scientific. Final.
6. PERFORMING ORG. REPORT NUMBER: ERP No. 711	
7. AUTHOR(s): R. Narcisi, L. Wlodyka, E. Trzcinski, P. Bench, G. Federico	8. CONTRACT OR GRANT NUMBER(s)
9. PERFORMING ORGANIZATION NAME AND ADDRESS: Air Force Geophysics Laboratory (LKD), Hanscom AFB, Massachusetts 01731	10. PROGRAM ELEMENT, PROJECT, TASK AREA & WORK UNIT NUMBERS: 61102F, 2310G301, 17, X64
11. CONTROLLING OFFICE NAME AND ADDRESS: Air Force Geophysics Laboratory (LKD), Hanscom AFB, Massachusetts 01731	12. REPORT DATE: 9 July 1980; NUMBER OF PAGES: 27
14. MONITORING AGENCY NAME & ADDRESS (if different from Controlling Office): I25AAH	15. SECURITY CLASS (of this report): Unclassified; 15a. DECLASSIFICATION DOWNGRADING SCHEDULE

16. DISTRIBUTION STATEMENT (of this Report)

Approved for public release; distribution unlimited.

17. DISTRIBUTION STATEMENT (of the abstract entered in Block 20, if different from Report)

18. SUPPLEMENTARY NOTES

19. KEY WORDS (Continue on reverse side if necessary and identify by block number)

Equatorial ionospheric irregularities
Spread F
Ionospheric holes
Rocket measurements
Ion composition
Ionospheric structure
Irregularities processes

20. ABSTRACT (Continue on reverse side if necessary and identify by block number)

Two multi-instrumented Terrier Malemute rockets including ion mass spectrometers were launched from Kwajalein on the nights of 17 and 23 July 1979 during equatorial Spread F events. Detailed ionospheric structure and composition measurements were made between about 100 and 590 km. The first flight penetrated six areas of "bite-outs" spread over the range 265 to 560 km on upleg as well as several more depletions on downleg. The strongest irregularities, up to 90 percent depletion, occurred at the altitudes of 265 to 285 km just above the F region ledge at 250 km. There was no evidence of

DD FORM 1 JAN 73 1473 EDITION OF 1 NOV 65 IS OBSOLETE

Unclassified

SECURITY CLASSIFICATION OF THIS PAGE (When Data Entered)

20. (Cont)

enhanced bottomside tracer ions (NO^+, O_2^+ or meteoric ions) in any of the holes, which were composed mostly of O^+ and smaller amounts of N^+. From the composition signatures, the source of the bubbles appeared to be near the F region ledge. Within the higher altitude holes, the N^+/O^+ ratios were smaller than the adjacent ionosphere ratios, indicating not only that the source regions were near the ledge, but also that the bubbles had initiated earlier when the ledge was at higher altitudes. While O^+ and N^+ exhibited strong fluctuations, NO^+ and O_2^+ had fairly smooth profiles with scale heights similar to N_2 and O_2 respectively, demonstrating steady-state conditions and a stable neutral atmosphere with an exospheric temperature of about 1100K. This suggests that neutral atmospheric turbulence is not a major source of the ionospheric irregularities. Time periods for ion-chemical processes to achieve the observed composition are discussed in terms of bubble formation times and rise velocities. The second flight showed an F region ledge near 350 km and irregularities only near the ledge, with O^+ dominating.

Preface

Support for this work was provided by the Air Force Office of Scientific Research under Task 2310G3 and by the Defense Nuclear Agency under Subtask I25AAHX640, Work Unit 06, Communications Effects Experiments.

Contents

Illustrations

Structure and Composition Measurements in Equatorial Ionospheric Bubbles

1. INTRODUCTION

The ion composition inside and outside equatorial depletions has been measured with satellite retarding potential analyzers and ion mass spectrometers.[1-4] Fe^+ ions were found to be either enhanced or depleted within the holes with the molecular ions (NO^+) oftentimes more abundant than O^+ which predominated outside the holes. Depletions in O^+ up to 10^3 have been observed. The bite-outs varied from a few kilometers to tens of kilometers in width.

The position of the F region ledge was generally unknown during the satellite measurements. In the equatorial region the ledge altitude could be greater than 450 km during certain times while outside this particular region the ledge could be at much lower altitudes. This would perhaps explain both the magnitude and shape

(Received for publication 8 July 1980)

1. Hanson, W. B., and Sanatani, S. (1971) Relationship between Fe^+ ions and equatorial spread F, J. Geophys. Res. 76:7761.

2. Hanson, W. B., and Sanatani, S. (1973) Large N_i gradients below the equatorial F peak, J. Geophys. Res. 78:1167.

3. Brinton, H. C., Mayr, H. G., and Newton, G. P. (1975) Ion composition in the nighttime equatorial F-region: Implications for chemistry and dynamics (abstract), EOS Trans, AGU 56:1038.

4. McClure, J. P., Hanson, W. B., and Hoffman, J. H. (1977) Plasma bubbles and irregularities in the equatorial ionosphere, J. Geophys. Res. 82:2650.

of some of the measured bite-outs, especially those of large scale, and the composition changes as well.

In order to determine equatorial irregularities processes more clearly it was recognized that detailed vertical profiles of the ionospheric plasma parameters were needed (as well as the satellite measurements), coincident with radar, ionosonde and neutral wind measurements. Such an effort, designated "PLUMEX" was conducted by the Defense Nuclear Agency.

The PLUMEX program, designed to measure equatorial ionospheric irregularities and their effects on communications channels and radar, was conducted at the Kwajalein Atoll (4.3°N dip latitude) during July 1979. As part of this effort two multi-instrumented Terrier Malemute rockets each with a plasma diagnostics complement of plasma probes, ion mass spectrometer, electric field sensors and a four-frequency beacon were flown during equatorial spread F events. The first rocket, PLUMEX 1, was launched 17 July (0031:30.25 local time) and the second, PLUMEX 2, 23 July (2157:30.4 local time). In this report we present the results from the ion mass spectrometer experiments only. We believe that these represent the first vertical profile measurements of the detailed ion mass composition and structure in equatorial ionospheric plumes.

2. INSTRUMENTATION AND MEASUREMENT PROGRAM

Figure 1 shows a schematic of the quadrupole ion mass spectrometer. The two important data outputs of the spectrometer were the total positive ion current collected on the aperture plate which was essentially a dc probe for ionospheric structure measurements and the mass spectra output for species composition. The mass program for the instrument is presented in Figure 2. Five mass numbers were sampled in sixteen sequences. Each programmed mass number was measured for 10 msec so that the total program period was 0.8 sec covering 80 separate mass numbers including mass repetitions for altitude resolution. The species associated with the mass numbers are $1(H^+)$, $4(He^+)$, $14(N^+)$, $16(O^+)$, contaminants from water vapor of $17(OH^+)$, $18(H_2O^+)$, and $19(H_3O^+)$, $23\ (Na^+)$, $24\text{-}25\text{-}26(Mg^+)$, $27(Al^+)$, $28(Si^+)$, $30(NO^+)$, $32(O_2^+)$ and $54\text{-}56(Fe^+)$. The remaining mass numbers were sampled to establish background levels. Between 110 and 588 km, the altitude resolution of the aperture plate output decreased from 1.5 to 0.2 m while that for the important ion species decreased from 150 to 20 m each varying with the vehicle velocity which diminished with increasing altitude. The instrument was mounted on the rocket axis at the forward end of the payload. The PLUMEX payload configuration and flight scenario are described in Figure 3.

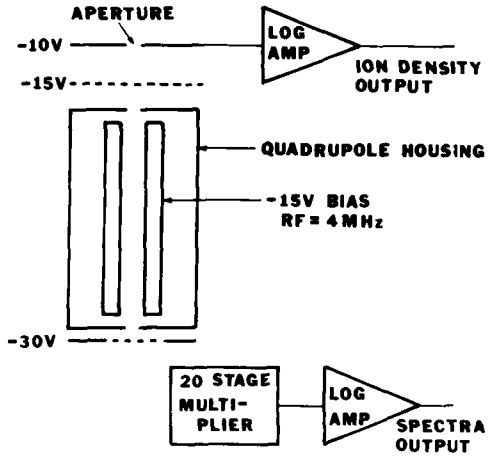

Figure 1. Schematic of the Quadrupole Ion Mass Spectrometer

MASS PROGRAM

SEQUENCE #	MASS # - AMU				
1.	1	4	14	16	30
2.	1	4	14	16	32
3.	14	16	28	54	56
4.	1	4	14	16	30
5.	1	4	14	16	32
6.	14	16	28	54	56
7.	1	4	14	16	30
8.	1	4	14	16	32
9.	14	16	28	54	56
10.	1	4	14	16	30
11.	1	4	14	16	32
12.	1	4	7	8	56
13.	13	14	15	16	17
14.	18	19	20	21	22
15.	23	24	25	26	27
16.	28	29	30	31	32

SAMPLE RATE: 10 MS/AMU

PROGRAM TIME: 0.8 SECONDS

Figure 2. Spectrometer Program for the Measurement of Selected Ion Mass Numbers at High Spatial Resolution

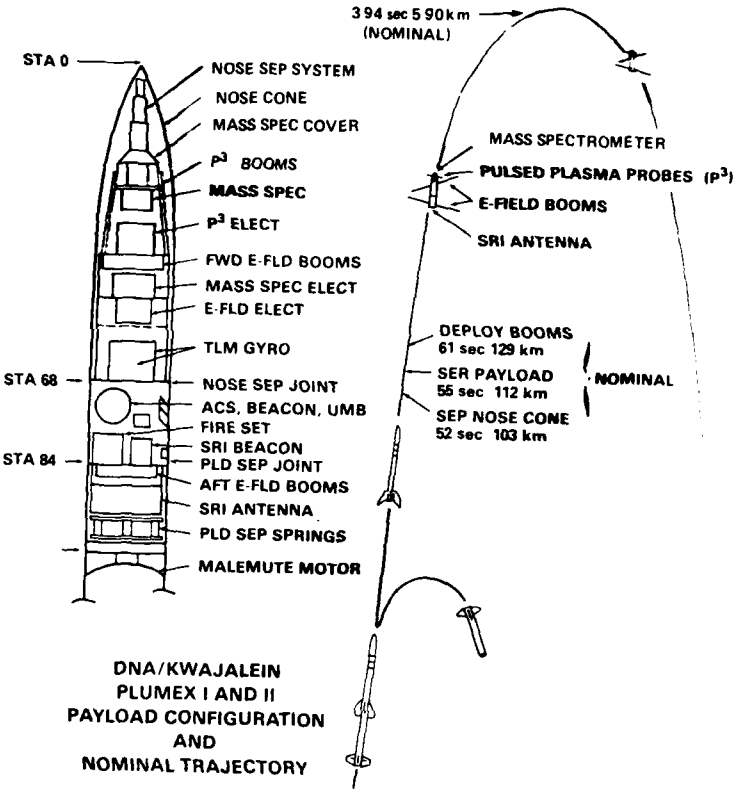

Figure 3. PLUMEX Payload Instrumentation and Flight Functions

3. MEASUREMENTS AND DISCUSSION

3.1 PLUMEX 1

Figure 4 shows the altitude versus current profiles of the aperture plate output (digitized at 2 khz and plotted) and the species of O^+, N^+, O_2^+ and NO^+ measured on ascent on PLUMEX 1. The positive spikes on the aperture current below 250 km and the negative spikes at higher altitudes are due to the nitrogen gas bursts from the attitude control jets. The rocket penetrated six areas of "bite-outs" in the F region. In no case was there any evidence of enhanced bottomside ions (NO^+, O_2^+ or meteoric ions). The steep F region ledge was created by O^+ ions which rose by more than three orders of magnitude over a space of less than 20 km. Estimated ion densities were about 6×10^5 ions/cc at the F peak and about 1100 ions/cc below the ledge with an accuracy of roughly a factor of 2.

NO^- measurements at higher altitudes where the NO^- was produced during the N_2 jet bursts by the reaction of $O^- + N_2 \rightarrow NO^- + N$ were not plotted in Figure 4.

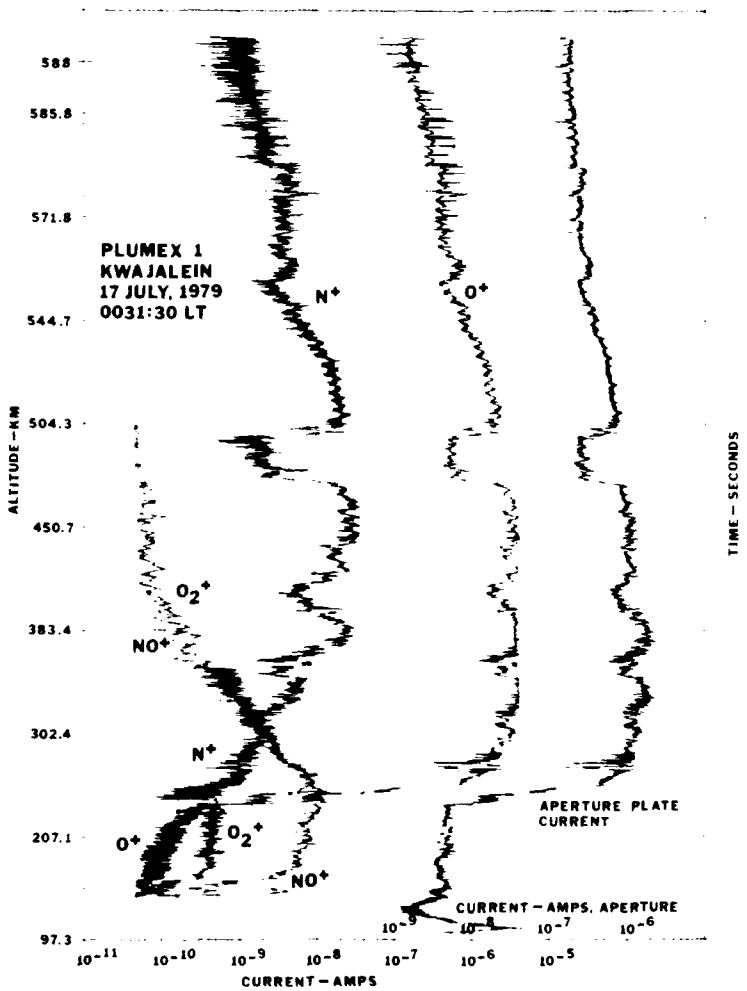

Figure 4. Ascent Measurements of PLUMEX 1 Showing the Aperture Plate, O^-, N^+, NO^+ and O_2^+ Current Profiles. Baseline current is 4×10^{-11} amps

The strongest ionospheric fluctuations with up to 90 percent depletion occurred between 265 and 285 km. An expanded plot of this region is given in Figure 5. Note

that the O^+ and N^+ ions generally follow the ionospheric fluctuations as depicted by the aperture plate current while NO^+ and O_2^+ do not. It can be shown that the NO^+ and O_2^+ have steady state distributions under the prevailing ionospheric conditions.

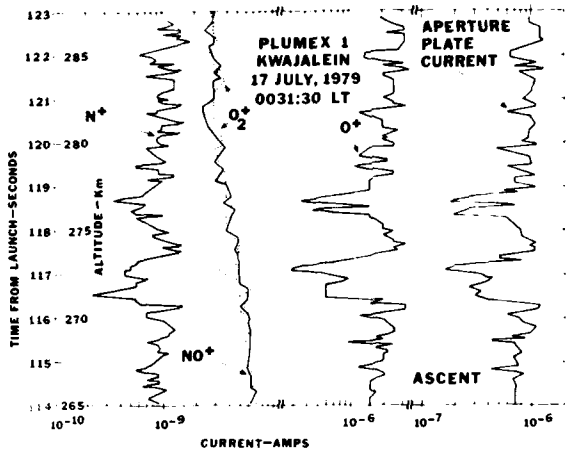

Figure 5. An Expanded Plot of the Strongest Irregularities in the Upleg 265 to 288 km Region. Note the relatively smooth molecular ion profiles. Meteoric ions were negligible

Figure 6 depicts the NO^+ and O_2^+ chemistry. Since the recombination coefficients (α's) and reaction rates (k's) vary mainly with temperature which is relatively constant over the altitude range 250 to 400 km, the NO^+ and O_2^+ concentrations should be directly proportional to the N_2 and O_2 concentrations respectively, as long as $\left[O^+\right] \approx N_e >> \left(\left[NO^+\right] + \left[O_2^+\right]\right)$. The molecular ions can achieve their steady state values in a relatively short time. An estimate of this time may be made by referring to Figure 5. Assuming first a zero order ionosphere and then the immediate removal of 90 percent of the plasma (the hole near 273 km) causing a 90 percent depletion in O^+, NO^+ and O_2^+. The time required for the molecular ions to return to their steady-state values by the chemistry in Figure 6 is approximately 8-9 minutes. Note that this time is not necessarily the age of the hole since it could have been in steady state longer nor is this time a lower limit on the hole's age because the hole may not have formed by an abrupt depletion mechanism. However, the NO^+ and O_2^+ distributions do indicate normal, relatively smooth N_2 and O_2 profiles, and this suggests that neutral atmospheric turbulence is not a major source for bottomside ionospheric plasma irregularities.

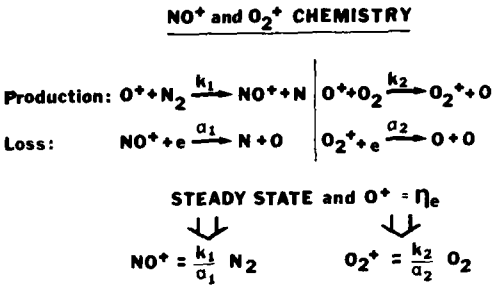

Figure 6. F Region Chemistry of NO^+ and O_2^+

In Figures 7 and 8 it is shown that the NO^+ and O_2^+ density profiles, and, in particular, the slopes calculated from N_2 and O_2 concentrations taken from the 1976 Standard Atmosphere match rather closely with the measured slopes. From the scale heights determined from slopes fit to the data an exospheric neutral temperature of 1100 ± 150K is inferred. Not only can the neutral concentrations of N_2 and O_2 be determined from the ion composition measurements but one can also determine the concentrations of N(4S) and NO from the bottomside ion composition as well.[5] This, however, will not be performed here.

Atomic nitrogen ions may perhaps be the more useful species for inferring ionospheric irregularities processes.[4] In Figure 5, N^+ shows similar irregularity structure as O^+. The presence of N^+ in this lower altitude range indicates the need for appreciable downward transport of N^+ since there are no significant chemical sources of N^+ at night and N^+ is rapidly destroyed in reactions with O_2. For example, the lifetimes of N^+ at 250 and 300 km are about 1 and 7 min, respectively. There was indeed a significant downward ionospheric drift of 10 m/sec as indicated by simultaneous radar observations.[6] Because both chemistry and ionospheric motions play equally important roles, the N^+ distribution can only be properly calculated with a detailed F region chemical-transport model. However, considering the short lifetimes of N^+, it is perhaps unlikely that the irregularity structure in Figure 5 is very much greater than 10 min old.

5. Anderson, D.N., and Rusch, D.W. (1980) Composition of the nighttime ionospheric F1 region near the magnetic equator, J. Geophys. Res. 85:2650.

6. Szuszczewicz, E.P., Tsunoda, R.T., Narcisi, R., and Holmes, J.C. (1980) Coincident radar and rocket observations of equatorial spread-F, Geophys. Res. Lett. (in press).

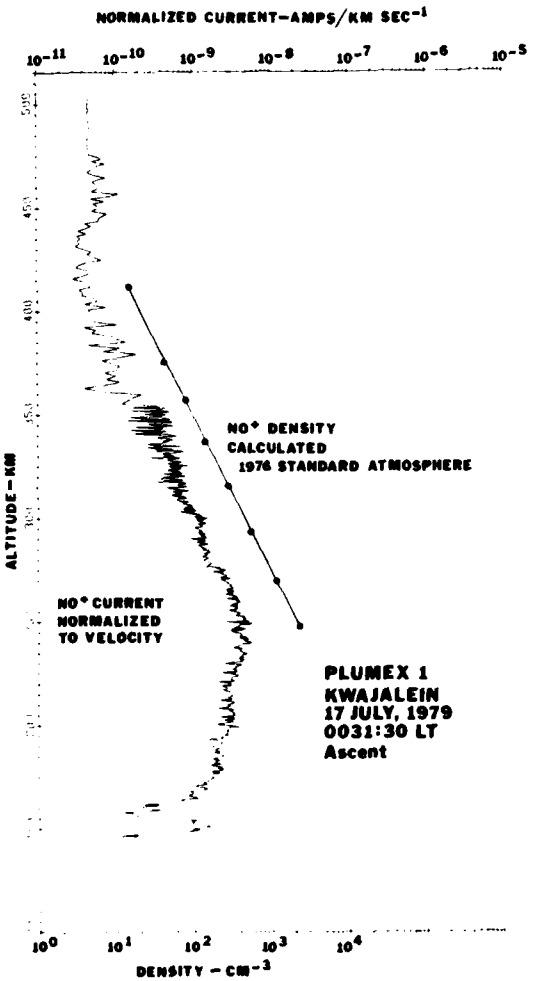

Figure 7. A Comparison of the Normalized NO^+ Current (Proportional to density) With a Calculated NO^+ density. The slope yields the N_2 scale height and temperature

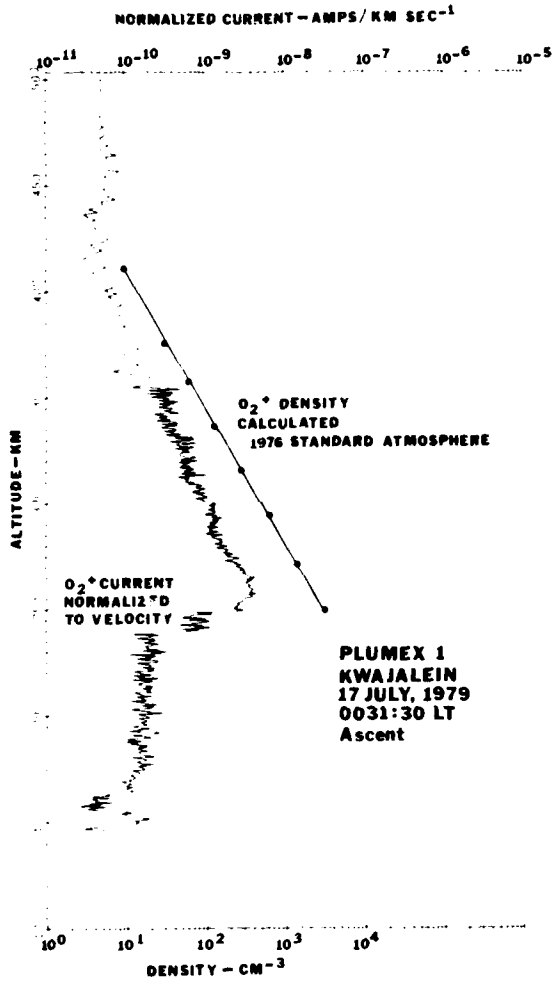

Figure 8. Similar to Figure 7 but for O_2^+. The O_2^+ calculated density profile must be reduced by a factor of 1.5 to yield the correct values

The N^+ distribution at higher altitudes also presents some interesting features as shown in the N^+/O^+ ratio versus altitude in Figure 9. It is seen that the N^+/O^+ ratio is considerably smaller in the large scale depletions than in the adjacent "zero order" areas. This and the magnitude of the O^+ and N^+ concentrations suggest that the depletions originated at or near the bottomside F region where $\left[O^+\right] \approx \left[O^+\right]_{\text{hole}}$. The radar data revealed that the large scale depletion at

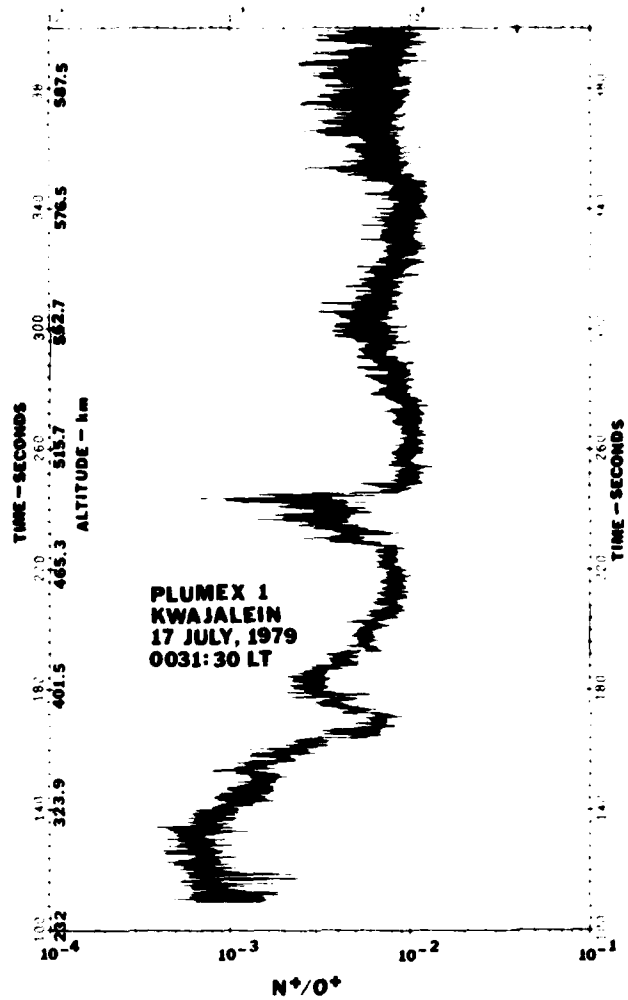

Figure 9. The N^+/O^+ Ratio on Ipleg Demonstrating the Diminished Ratios in the Holes

475 to 500 km was at nominal altitude for more than 30 min and that its upward rise velocity was essentially zero.[7] Further, the radar measurements indicated that spread F occurred shortly after ionospheric motion reversal from upward to downward when the F region ledge was at much higher altitudes.[7] Thus, while it is still correct that the ion composition indicates that the source region of this bubble

7. Tsunoda, R.T. (private communication)

was at or near the F region ledge, the ledge was probably at much higher altitudes than 250 km when these bubbles formed. The picture here seems to be that the bubbles are somewhat continuously generated near the ledge and then move upward while the ledge is drifting downward during the night. Our particular rocket launch took place when the irregularities were in the decay phase which is defined as the period after the depletion's upward motion has stopped.

If the radar measurements were unavailable and it was presumed that the 475 to 500 km depletion originated near 262 km where similar O^+ concentrations prevailed, one can calculate an upper limit of the bubble vertical drift velocity by utilizing the source region levels of NO^+ and O_2^+. The molecular ion concentrations in the source region are not preserved at higher altitudes because of losses by dissociative recombination and a simultaneous loss in production by ion-atom interchange and charge exchange reactions since $\left[N_2\right]$ and $\left[O_2\right]$ decrease markedly with altitude. The longer it takes a bottomside depletion to move upward, the more likely the elimination of molecular ion signatures when $\left[O^+\right] \approx N_e >> \left(\left[NO^+\right] + \left[O_2^+\right]\right)$. In the case of the 475 to 500 km depletion, a vertical transport time somewhat greater than 360 sec would account for the molecular ion deficiency. This estimate is based on an instantaneous displacement of the bottomside ion composition to the 475 to 500 km range and a calculation showing that in about 6 min the molecular ion levels would be comparable to the ones in the depletion. This time estimate would then suggest an upper limit of about 600 m/sec for the depletion's average vertical drift velocity. However, the radar measurements showed the bubble was essentially stopped for some time and, considering the short lifetime of N^+ in the lower altitude region near 275 km, it is unlikely that the lower altitude N^+ levels could be maintained if the source region was at this low altitude with the bubble subsequently rising to about 500 km even if the upward drift velocity was 600 m/sec. Further the $\left[N^+\right]$ in the higher altitude hole is somewhat larger than in the source region where $\left[O^+\right] \approx \left[O^+\right]_{hole}$. Although the O^+ in the source would be essentially preserved during the upward traversal time, N^+ would not and would certainly show a decay. This all indicates that the source region for the 475 to 500 km hole was indeed at the ledge, but when this ledge was at higher altitudes where the N^+ concentrations could endure. The exact altitude of the ledge is also dependent on the bubble's vertical velocity; a faster upward drift means the bubble could have initiated at lower heights.

Meteoric species measured on PLUMEX 1 are shown in Figure 10. Iron and magnesium ions were present up to 180 km with peak concentrations of up to about 100 ions/cc. Meteoric ions, mainly Mg^+, were detected at much higher altitudes but only in concentrations of 5-10 ions/cc.

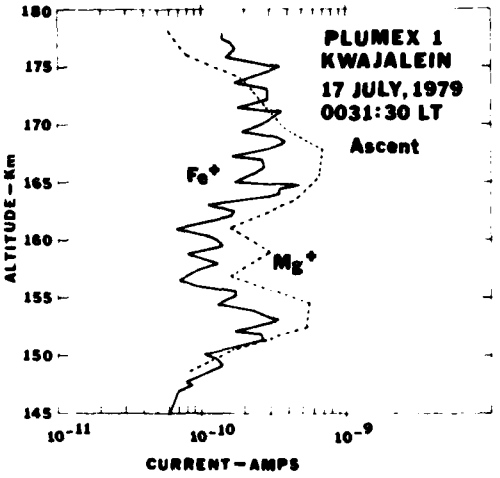

Figure 10. Meteoric Species Measured on Upleg, Mg^+ Was Also Detected at Higher Altitudes With Peak Currents in the Vicinity of 4×10^{-11} amps

Figure 11 shows the contaminant species, OH^+(17) and H_2O^+(18), which were about 1 percent of the total plasma density. The H_2O^+ ions are produced through the rapid charge transfer reaction of O^+ with H_2O outgassing from the rocket. This had only a very small affect on the ambient species measurements. It is not clear how the OH^+ ion was produced; since the O^+ reaction with H_2O to produce OH^+ is slightly endothermic.

Figure 12 presents the NO^+/O_2^+ ratio exhibiting values of 10 to 20 in the F1 region and rapidly decreasing at the ledge to a steady value of 1 ± 0.2 from 260 to 450 km.

Finally, Figure 13 shows the upleg and downleg aperture current measurements. The negative spikes on descent are due to the attitude control system's N_2 gas bursts. Note that there are several depletions seen on downleg also and that the ledge is about 25 km lower.

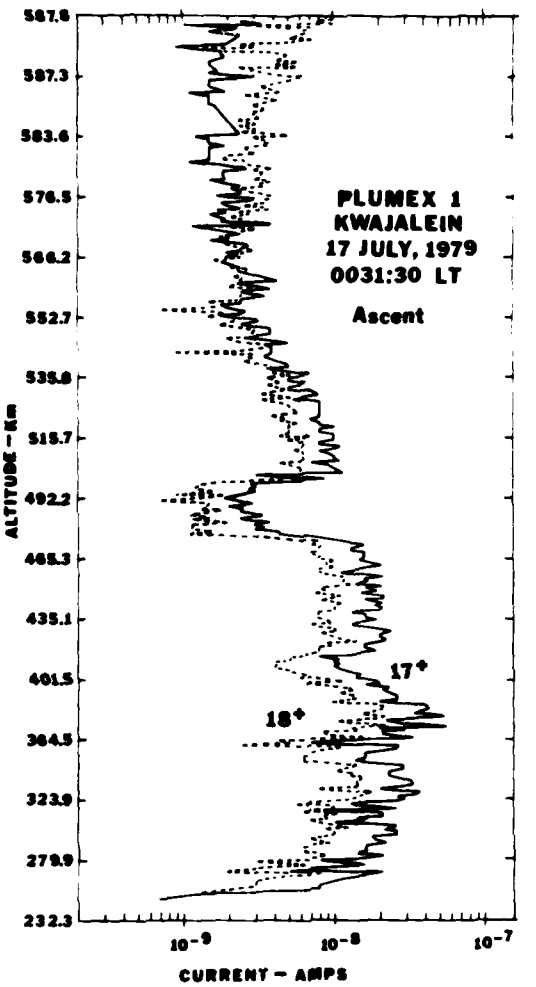

Figure 11. Contaminant Ions of OH^+ and H_2O^+ Measured on Upleg

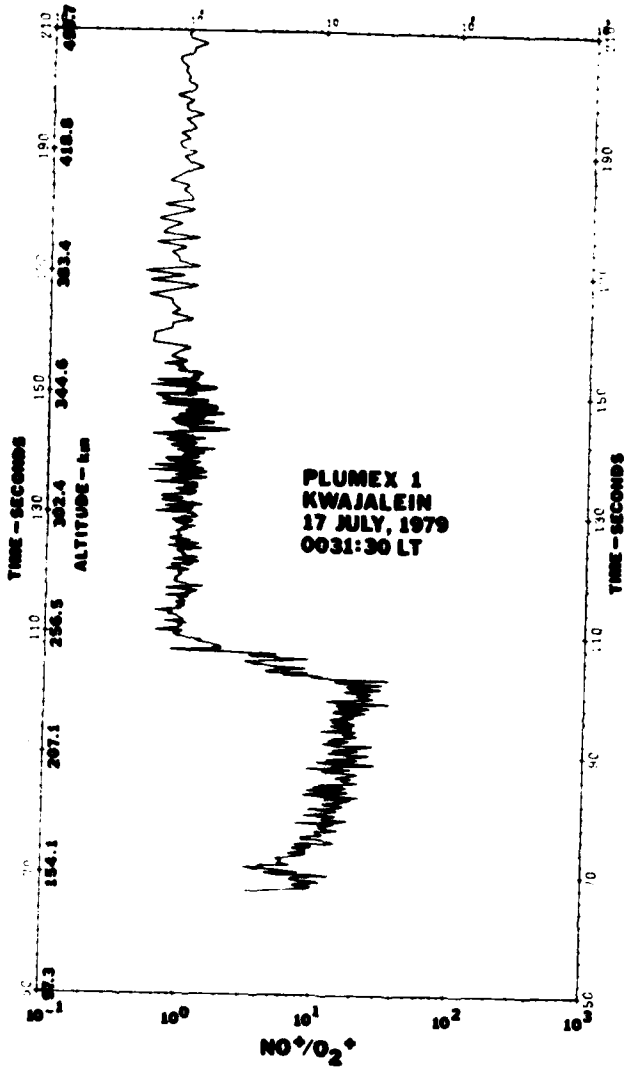

Figure 12. The NO^+/O_2^+ Ratio on Ascent

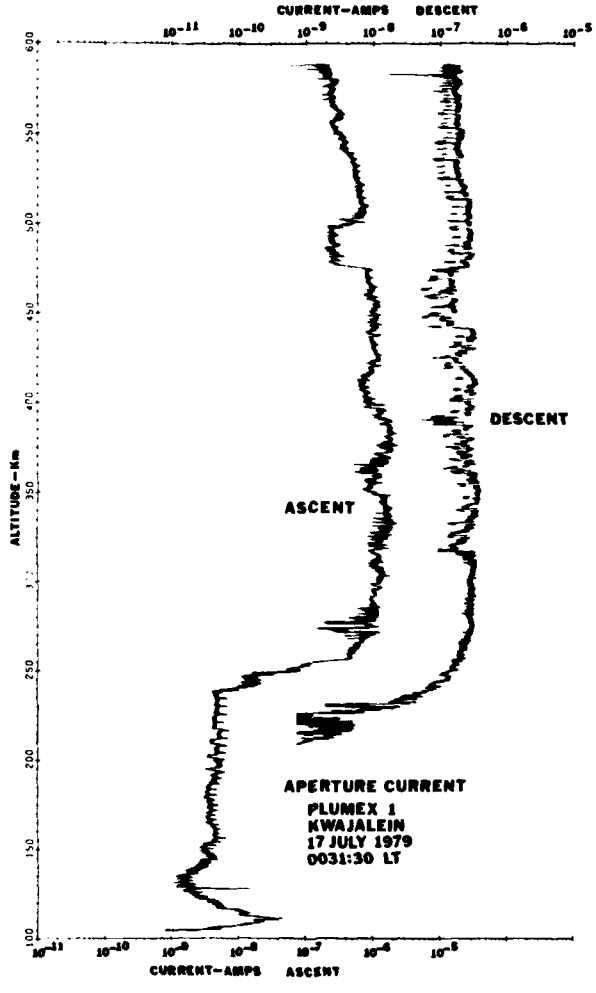

Figure 13. A Comparison of the Ascent and Descent Aperture Plate Current Measurements Showing Several Depletions Penetrated on Descent

3.2 PLUMEX 2

The PLUMEX 2 payload was launched six days later and about 2-1/2 hr earlier in the evening. Figure 14 shows the altitude versus current ascent measurements of the aperture plate output and the species, O^+, N^+, NO^+ and O_2^+. In this flight the payload did not separate from the rocket motor which rendered the attitude control system ineffective. The vehicle's attitude was stable up to 300 km above which the angle of the attack increased and varied causing the modulations in the data. Nevertheless the F region ledge is now seen to be near 350 to 360 km. If a 10 m/sec downward drift was still prevalent, then this ledge would appear near that of PLUMEX 1, 2-1/2 hr later, the time of the PLUMEX 1 launch.

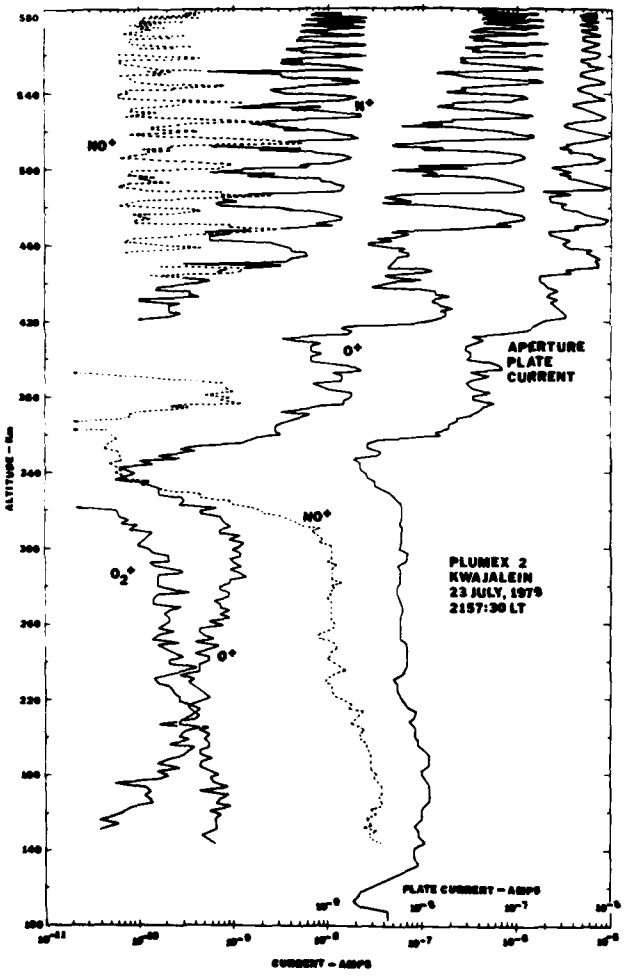

Figure 14. Ascent Measurements of PLUMEX 2 Presenting the Aperture Plate, O^+, N^+, NO^+ and O_2^+ Current Profiles. Only a portion of the data (points every 0.8 sec) was used to generate the profiles. The vehicle became unstable above 300 km, the variations in aspect causing the current modulations.

Figure 15 presents the upleg and downleg measurements of the aperture plate current. The irregularities, especially those of smaller scale between 350 and 400 km, cannot be entirely explained by vehicle aspect modulations and are probably real, representative of bottomside Spread F. The descent measurements depict a quiet, unperturbed ionosphere.

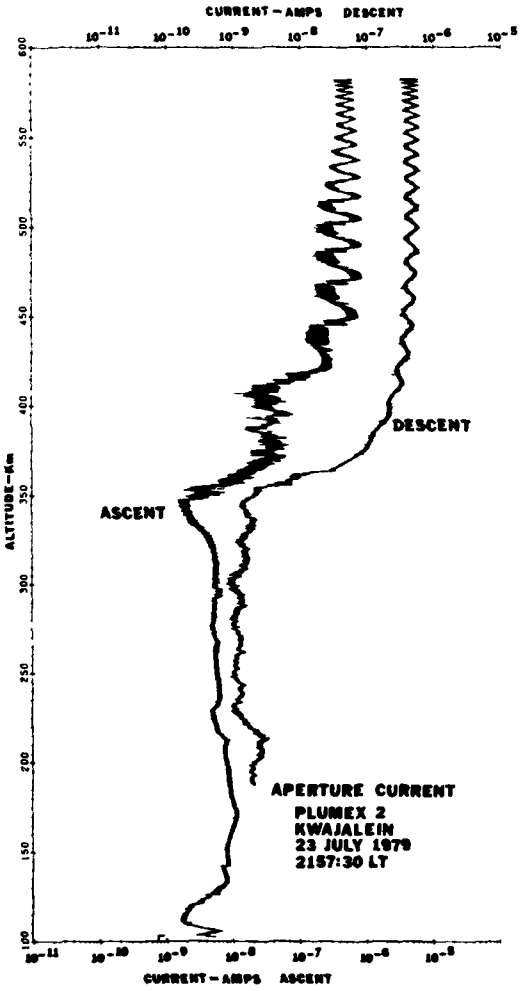

Figure 15. A Comparison of the Ascent and Descent Aperture Plate Current Profiles. The descent profile depicts a quiescent ionosphere

The meteoric species measured on PLUMEX 2 are shown in Figure 16. Significant concentrations of iron and magnesium ions are seen in layers up to 260 km, about 80 km higher than PLUMEX 1. These species were perhaps moved to higher altitudes by earlier upward ionospheric drift and essentially remained there because the downward motion after ionospheric drift reversal was not operative long enough to drag them to lower altitudes.

All these data are still in the process of reduction and analysis. Descent species measurements, current-density conversions, and removal of the aspect modulation in PLUMEX 2 remain to be performed. Finally these data need to be fit to an F region chemical-transport model from which detailed irregularities processes may be determined.

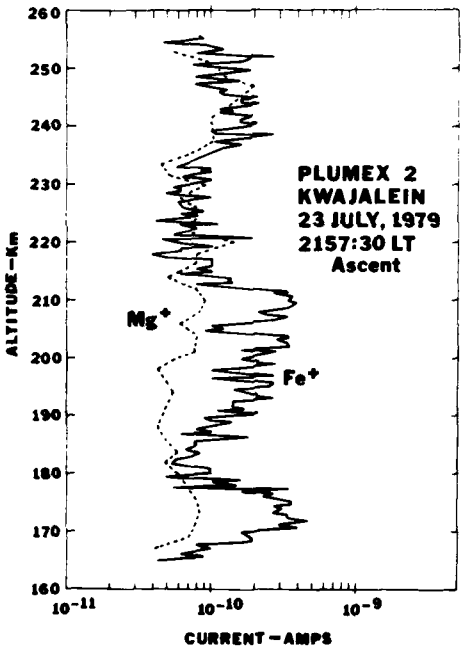

Figure 16. Meteoric Species Measured on Ascent

4. CONCLUSION

A considerable amount of information on ionospheric plumes and processes can be obtained from ion composition and structure measurements during such events. Preliminary analysis of the results leads to the following comments and conclusions:

(a) The measurements clearly demonstrated that not all holes contain enhanced bottomside molecular and metal ion species, indeed none of the holes had such signatures,

(b) The composition signatures not only proved the depletion's source region to be at or near the F region ledge but also can be used to determine the altitude of the ledge at the time of depletion formation,

(c) Evidence was presented from the molecular ion distributions that showed a stable neutral atmosphere in the simultaneous presence of strong ionospheric fluctuations suggesting that neutral atmospheric turbulence is not a major source of bottomside plasma irregularities,

(d) From the ion composition measurements, it is possible to derive N_2, O_2, N(4S) and NO neutral concentrations as well as the atmospheric neutral temperature,

(e) Utilizing the composition measurements and ion chemistry, one can estimate limits on bubble lifetimes and rise velocities under certain conditions.

(f) Finally, the in-situ measurements along with the radar measurements of ionospheric motions will allow a more detailed determination of ionospheric irregularities processes when coupled to F region chemical-transport model calculations.

References

1. Hanson, W. B., and Sanatani, S. (1971) Relationship between Fe^+ ions and equatorial spread F, J. Geophys. Res. 76:7761.
2. Hanson, W. B., and Sanatani, S. (1973) Large N_i gradients below the equatorial F peak, J. Geophys. Res. 78:1167.
3. Brinton, H. C., Mayr, H. G., and Newton, G. P. (1975) Ion composition in the nighttime equatorial F-region: Implications for chemistry and dynamics (abstract), EOS Trans, AGU 56:1038.
4. McClure, J. P., Hanson, W. B., and Hoffman, J. H. (1977) Plasma bubbles and irregularities in the equatorial ionosphere, J. Geophys. Res. 82:2650.
5. Anderson, D. N., and Rusch, D. W. (1980) Composition of the nighttime ionospheric F1 region near the magnetic equator, J. Geophys. Res. 85:569.
6. Szuszczewicz, E. P., Tsunoda, R. T., Narcisi, R., and Holmes, J. C. (1980) Coincident radar and rocket observations of equatorial spread-F, Geophys. Res. Lett. (in press).
7. Tsunoda, R. T. (private communication).